Ashdin Publishing
Biosensors Journal
Vol. 1 (2012), Article ID H110601, 7 pages
doi:10.4303/BJ/H110601

Research Article

Anti-Prostate Specific Antigen (Anti-PSA) Modified Interdigitated Microelectrode-Based Impedimetric Biosensor for PSA Detection

Sunil K. Arya and Shekhar Bhansali

Bio-MEMS and Microsystems Laboratory, Department of Electrical Engineering, University of South Florida, 4202 E. Fowler Avenue, ENB 118, Tampa, FL 33620, USA
Address correspondence to Sunil K. Arya, sunilarya333@gmail.com

Received 9 June 2011; Revised 23 August 2011; Accepted 24 August 2011

Abstract Interdigitated microelectrodes (IDEs) functionalized with a cysteamine (Cys) self-assembled monolayer (SAM) were used to fabricate a sensitive, disposable, impedimetric biosensor for prostate specific antigen (PSA) detection. PSA specific monoclonal antibody (anti-PSA) was covalently immobilized on cysteamine modified gold surface of IDEs, using N-ethyl-N'-(3-dimethylaminopropyl) carbodiimide and N-hydroxysuccinimide (EDC/NHS) chemistry. Bovine serum albumin (BSA) was used as a blocker to prevent nonspecific adsorption on electrode surface. BSA-anti-PSA/Cys/IDE electrodes were exposed to solutions with different PSA concentrations and their response was measured using a label-free electrochemical impedance (EIS) technique. The impedance changes revealed close a correlation with PSA concentrations in the measurement range of $1\,\text{pg.mL}^{-1}$–$100\,\text{ng.mL}^{-1}$, with sensitivity of $0.444\,\text{mL.g}^{-1}$.

Keywords prostate cancer; self-assembled monolayer; electrochemical impedance; interdigitated microelectrodes; biosensor

1 Introduction

Over the past two decades, biosensors have revolutionized the point-of-care diagnosis [36]. Among the point-of-care devices, biosensors based on electrochemical detection techniques continue to be of great interest for operational simplicity, affordability, shelf life, selectivity and sensitivity [4,30]. Electrical impedance spectroscopy (EIS)-based biosensors are a class of electrochemical biosensors that allows the label free recording of interaction between bio-recognition element and analyte occurring at the electrode surfaces and can be measured in form of changes in capacitance and/or resistance [27]. EIS measurements can be carried out over a frequency range or at a single frequency by applying a small sinusoidal voltage (perturbation voltage). The use of small perturbation voltage for response measurement also helps to minimize matrix interference [5, 22,16]. The current-voltage ratio provides the frequency-dependent impedance and is used to study the changes at the electrode-solution interface [2,7,8]. An EIS-based biosensor using interdigitated microelectrodes (IDEs) offers additional advantages of rapid reaction kinetics, improved sensitivity, large electrode aspect ratio (w/l) and increased signal-to-noise ratio [16,27,34,37]. An interdigitated microelectrode (IDE) (with, electrodes containing parallel microband with alternating microbands connected together) is a two-electrode system possessing enhanced mass transport properties with reduced IR drop and double-layer charging effects that help to attain steady-state current responses faster than three or four electrode systems, enabling easier measurements [20,23,35]. Furthermore, for response measurement, they do not require third reference electrode, thus making the system simpler for realization of products. It has recently been shown that IDE-based systems with EIS can be used for the estimation of cortisol [1], avian influenza virus H5N1 [37], atrazine [27,28,34] and bacterial cells [35]. However, no such efforts have been made to detect cancer biomarkers, which need to be detected at significantly lower concentrations.

Prostate cancer (PCa) is one of the leading causes of cancer morbidity [15]. At present, once PCa spreads beyond the limits of an organ; there is no curative treatment available. Like most cancers, early detection continues to be critical for reduced mortality from PCa [25]. A specific biomarker-based sensing can enable the detection of the unique association of genomic changes in cancer cells with the disease process. A biomarker-based sensing continues to be an active area of research and offers a reliable and affordable approach towards diagnostics. Prostate specific antigen (PSA), a 32–33-kDa single-chain glycoprotein, has been extensively studied in the past decades and is a reliable and widely used tumor maker for the early detection of organ confined PCa [11,19,26,29,32]. In prostate cancer diagnosis, a PSA measurement above $10.0\,\text{ng.mL}^{-1}$ is regarded as positive and indicates a high probability of

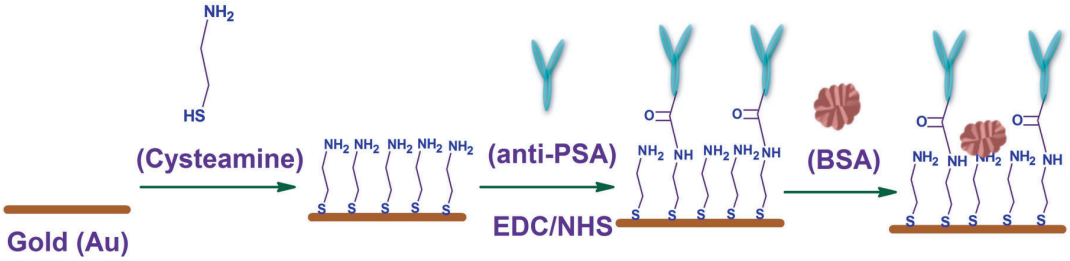

Figure 1: Schematic of BSA-anti-PSA/Cys/IDE electrode fabrication.

prostate cancer; below $4.0\,\text{ng.mL}^{-1}$ the result is considered negative and indicates a low probability of prostate cancer; between $4.0\,\text{ng.mL}^{-1}$ and $10.0\,\text{ng.mL}^{-1}$ the result is in the so-called "grey zone" and free PSA/total PSA ratio indicates cancer specificity; ratios above 0.25 indicate low risk of prostate cancer [9]. Hence, its detection at early stages can provide a significant impact on reducing patient mortality.

A commercial kit-based enzyme-linked immuno assay (ELISA) and its variants are currently the predominant analytical technique for a quantitative analysis of PSA. Some of the currently available analyzer-run PSA assays in market are from Abbott Diagnostics, Diagnostic Product Corporation, Roche, Beckman Coulter, Bayer Diagnostics and so on. These reliably detect PSA up to the range of 0.05–$0.005\,\text{ng.mL}^{-1}$ [12]. They provide a sensitive estimation of PSA; however, the techniques tend to be laborious, lengthy, expensive and are mainly confined to dedicated centralized laboratories using large, automated analyzers and trained personnel [12]. As approaches are sought for point-of-care patient management, various biosensor strategies based on surface plasma wave [32], surface plasmon-enhanced fluorescence [38], chemiluminescence [39], nanomechanical cantilever [14,17], surface enhanced resonance raman scattering [31] and electrochemical [6,9, 10,21,24,26] have been attempted for PSA detection. Each of the above has its advantages; however, EIS being the electrochemical, label-free and simple technique has shown a promise for the development of label-free ultrasensitive sensor [1,10,28,35].

This research demonstrates the use of anti-PSA modified IDEs to function as a simple, sensitive and disposable impedimetric biosensor chip for PSA detection. Cysteamine was used to prepare a self-assembled monolayer (SAM) on the IDEs' surface. The SAM was then used for the covalent binding of anti-PSA using N-ethyl-N'- (3-dimethylaminopropyl) carbodiimide and N-hydroxysuccinimide (EDC/NHS) chemistry [3]. The use of cysteamine and EDC/NHS activated the binding of anti-PSA results in covalent binding between amino group of cysteamine and carboxylic group of anti-PSA. Such binding leaves both active sites (upper NH_2 terminal end in Y-shaped antibody) of anti-PSA free for PSA recognition, and thus it improves the sensitivity of the system (Figure 1). A label-free impedimetric technique has been employed for PSA detection. The novel biosensor enabled PSA detection down to $1\,\text{pg.mL}^{-1}$ with a 30 min of incubation time.

2 Materials and methods

2.1 Chemicals and reagents

Monoclonal PSA antibody (anti-PSA, product number MCA2561), PSA (product number 7820-0504) and monoclonal cortisol antibody (product number 2330-4809) were procured from Abd Serotec. Cysteamine hydrochloride, EDC, NHS and phosphate buffered saline (PBS) tablets were purchased from Sigma Aldrich. PBS-tween tablets were purchased from Fluka. SU-8 resist was purchased from MicroChem Corp. All other chemicals were of analytical grade and were used without further purification. PBS solution ($10\,\text{mM}$, pH 7.4) was prepared by dissolving 1 tablet in $200\,\text{mL}$ of deionized water and PBS-tween solution ($10\,\text{mM}$ PBS, pH 7.4 containing 0.05% tween) was prepared by dissolving 1 tablet in $500\,\text{mL}$ water. Working solutions of PSA, anti-PSA and anti-cortisol were prepared by dilution in PBS ($10\,\text{mM}$, pH 7.4).

2.2 Measurement and apparatus

Electrochemical impedance spectroscopy (EIS) was utilized to characterize the BSA-anti-PSA/Cys/IDE electrodes and to estimate PSA concentration. EIS measurements were carried out at equilibrium potential (open circuit potential generated between electrodes dipped in electrolyte), without external biasing in the frequency range of 10–10^5 Hz, with a $25\,\text{mV}$ amplitude using Autolab Potentiostat/Galvanostat (Eco Chemie, Netherlands). EIS measurements were carried out using $60\,\mu\text{L}$ of PBS solution ($10\,\text{mM}$, pH 7.4) containing a mixture of $5\,\text{mM}$ $Fe(CN)_6^{4-}$ (Ferrocyanide) and $5\,\text{mM}$ of $Fe(CN)_6^{3-}$ (Ferricyanide), that is, $5\,\text{mM}$ $Fe(CN)_6^{3-/4-}$ as a redox probe.

2.3 Test chip fabrication

The IDE chips were fabricated on an oxidized $4''$ silicon wafer using standard photolithographic techniques [1,2].

A 5 μm wide and 3200 μm long electrode bands with 10 μm spacing, distributed over 5500 μm length, were lithographically transferred on the Si wafer. Next, Cr/Au (20/200 nm) was deposited using e-beam evaporation and the resist stripped. The resulting metal liftoff resulted in the IDE pattern. As a final step, SU8 chambers of about 50 micron thick were patterned around the electrodes, using the SU8 50 to create a sample well around these electrodes. SU8 was hard baked at 200 °C to improve its resistance against hard solvents like acetone.

2.4 SAM preparation and anti-PSA immobilization

The IDE chips were pre-cleaned with acetone, isopropyl alcohol and deionized water, and immersed in 1 mg.mL^{-1} solution of cysteamine in water. IDE chips in cysteamine solution were kept overnight at room temperature for self-assembled monolayer (SAM) formation. The cysteamine SAM modified electrodes were then rinsed with water to remove any unbound cysteamine and utilized for antibody immobilization. Anti-PSA was covalently attached to cysteamine SAM using EDC/NHS chemistry (Figure 1). For covalent binding, 30 μL of anti-PSA solution (1 μg.mL^{-1}) containing 0.4 M EDC and 0.1 M NHS was poured onto cysteamine modified IDE chips and kept for 1 h and 30 min in humid chamber at room temperature. Chips were kept in humid chamber to prevent drying of surface during anti-PSA binding. Anti-PSA immobilization occurs via a coupling reaction between the amino group of cysteamine and the EDC/NHS activated carboxylic group of anti-PSA. The electrode (anti-PSA/Cys/IDE) formed was washed thoroughly with PBS-tween (10 mM, pH 7.4) to remove any unbound anti-PSA. In the final step, BSA solution (10 μg.mL^{-1}) in PBS (10 mM, pH 7.4) was used to block nonspecific adsorption onto the electrode surface. The fabricated BSA-anti-PSA/Cys/IDE electrodes were characterized by using the electrochemical impedance technique and utilized for PSA estimation. Each experiment was run in triplicates and represented with error bars. Figure 1 schematically illustrates BSA-anti-PSA/Cys/IDE electrode fabrication.

3 Results and discussion

3.1 Electrochemical impedance studies

EIS studies are well-established and known for characterization of an electrode-solution interface. EIS studies reveal charge transfer processes occurring at the electrode-solution or modified electrode-solution interfaces. Any change in the EIS spectra can be related to the change in interface properties, thus can be utilized for surface modification characterization. In the present study, Nyquist plots were utilized to study (i) the change in charge transfer resistance (R_{ct}) at sensor-solution interfaces after cysteamine SAM formation, anti-PSA binding and BSA blocking and (ii) the change of charge resistance, with changing concentration of PSA. All EIS spectra were recorded in PBS (10 mM, pH 7.4) containing 5 mM $Fe(CN)_6^{3-/4-}$ as a redox probe.

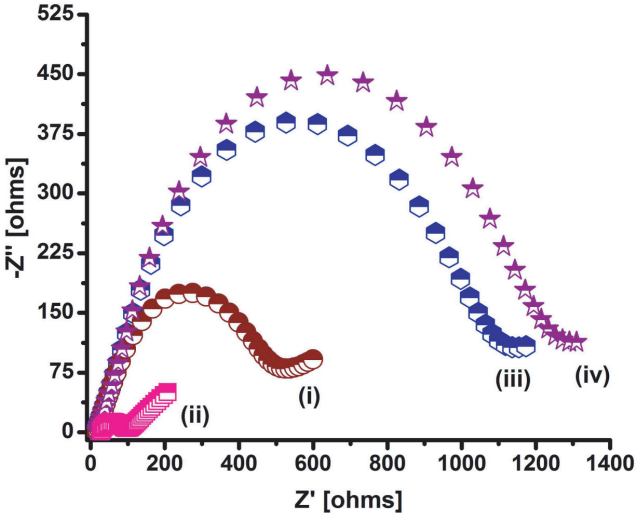

Figure 2: Nyquist plots of (i) blank IDE electrode, (ii) Cys/IDE electrode, (iii) Anti-PSA/Cys/IDE electrode and (iv) BSA-anti-PSA/Cys/IDE electrode.

3.1.1 BSA-anti-PSA/Cys/IDE electrode fabrication

Figure 2 shows the Nyquist plots of impedance spectra measured on the IDE surface after each modification process. In these spectra, the diameter of a semicircle represents the charge transfer resistance (R_{ct}) on the electrode surface. Cysteamine SAM formation on IDE is indicated by the decrease in R_{ct} from 474 Ω (Figure 2, curve (i)) to 90 Ω (Figure 2, curve (ii)). The decrease can be attributed to the presence of a large number of polarizable amino groups on the surface, which attracts the negatively charged redox molecules and facilitates the charge transfer to electrode surface [3]. In Figure 2, curve (iii), the increase in R_{ct} to 1048 Ω suggests the binding of anti-PSA onto the cysteamine SAM. The increase in R_{ct} can be attributed to the non-conducting nature of anti-PSA protein that resists the charge transfer from solution to the electrode. Finally, the increase in R_{ct} to 1178 Ω (Figure 2, curve (iv)) after treatment with BSA can be attributed to the BSA protein binding and blocking of the free spaces on the electrode.

3.1.2 PSA response studies of BSA-anti-PSA/Cys/IDE electrode

BSA-anti-PSA/Cys/IDE electrode was utilized to study the interaction between immobilized anti-PSA and PSA concentrations (1 pg.mL^{-1}–100 ng.mL^{-1}) (Figure 3). Figure 3 illustrates the Nyquist plots, that is the graph

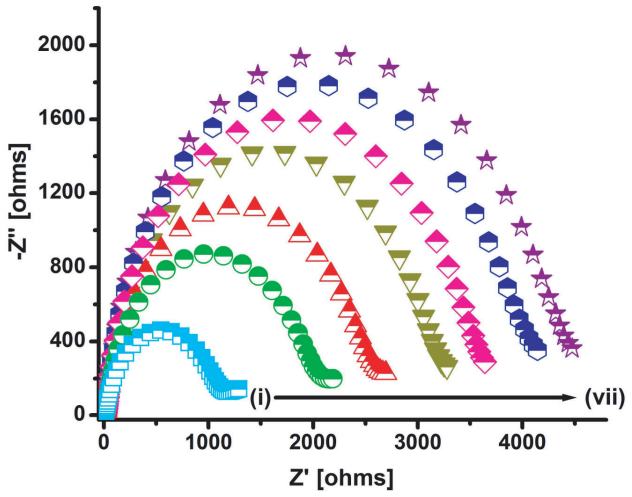

Figure 3: Nyquist plot of BSA-anti-PSA/Cys/IDE electrode for PSA concentration (i) buffer, (ii) $1\,\mathrm{pg.mL^{-1}}$, (iii) $10\,\mathrm{pg.mL^{-1}}$, (iv) $100\,\mathrm{pg.mL^{-1}}$ (v) $1\,\mathrm{ng.mL^{-1}}$, (vi) $10\,\mathrm{ng.mL^{-1}}$ and (vii) $100\,\mathrm{ng.mL^{-1}}$.

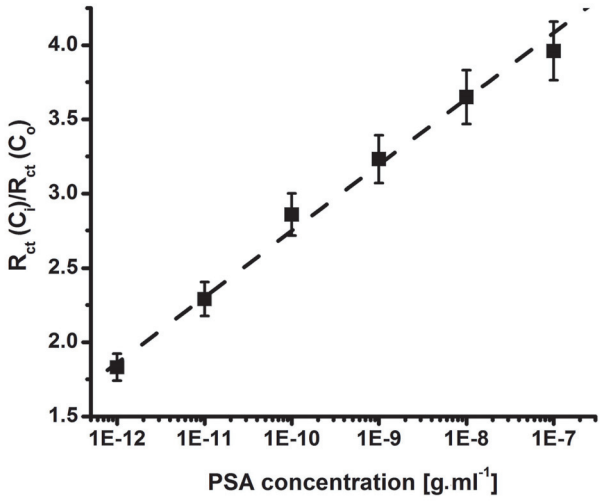

Figure 4: Normalized data curve for data obtained from R_{ct} data for different PSA concentrations.

between real part of impedance (Z') and imaginary part of impedance ($-Z''$) obtained upon a gradual increase of PSA concentration. For each concentration, the electrode was incubated in PSA solution for 30 min, followed by PBS-tween washing and EIS spectra recording in PBS (10 mM, pH 7.4) containing 5 mM $Fe(CN)_6^{3-/4-}$. From Figure 3, it is clear that charge transfer resistance (R_{ct}) increases regularly with increasing PSA concentration. The increase in R_{ct} is attributed to the binding of PSA protein molecules to immobilized anti-PSA on the electrode, producing an insulating layer that decreases the charge transfer for the redox probe.

For sensing applications, measurement of relative change in R_{ct} carries more significance than absolute R_{ct} value, and has been used for PSA estimation. To account for the variation in initial impedance values, due to the lack of industrial scale process control and the amount of antibodies and BSA binding on electrode surface, all experiments were carried out with increasing PSA concentration. The resulting R_{ct} data set was normalized to (R_{ct} for desired concentration (R_{ct} (C_i)))/(R_{ct} of blank BSA-anti-PSA/Cys/IDE electrode (R_{ct} (C_o))). The use of step-by-step approach ensured that the observed change in impedance was due to surface modification occurring by PSA binding and not due to superimposed effects of multielectrode measurement. Further with normalization, results of different electrodes were found to fall within 5% error range for different electrodes. In Figure 4, the graph of (R_{ct} (C_i))/(R_{ct} (C_o)) versus that of PSA concentration indicates the linear detection range of $1\,\mathrm{pg.mL^{-1}}$–$100\,\mathrm{ng.mL^{-1}}$, with the detection limit of $1\,\mathrm{pg.mL^{-1}}$. Normalized data curve in Figure 4 can be characterized using R_{ct} (C_i)/R_{ct} (C_o) $= 7.20 + 0.444\ C_{PSA}$, with a correlation coefficient of 0.997, and sensitivity of $0.444\,\mathrm{mL.g^{-1}}$. Further, studies reveal that after normalization, all electrodes with different impedances for BSA-anti-PSA/Cys/IDE exhibited a similar response within a 5% error for each concentration.

A curve between frequency and imaginary part of impedance ($-Z''$) and another between frequency and real part of impedance (Z') have also been analyzed at 50 Hz. Results suggested the similar linear behavior using these parameters (Z' and $-Z''$) and can thus also be utilized for sensing applications.

3.2 Estimation of association constant for interaction between the covalently bound anti-PSA and PSA

Association constant (K_a) was estimated using EIS data to check the interaction affinity of covalently bound anti-PSA with PSA antigen. EIS data analysis does not directly provide data on the amount of molecules adsorbed on the electrode surface, thus another method is required. For K_a estimation, Szymanska et al. [33] and Li et al. [18] showed that the Langmuir isotherm approach, where isotherm assumes equal binding energy for all binding sites, can be utilized for the estimation of K_a for binding interaction. They demonstrated that the change in charge transfer resistance (R_{ct}) may be related to the binding of target with immobilized molecule and the following equation can be used to evaluate K_a:

$$K_a C = \frac{R_{ct}(C_i) - R_{ct}(C_o)}{R_{ct}(C_o)} = \frac{\Delta R_{ct}(C_i)}{R_{ct}(C_o)}, \qquad (1)$$

where K_a is the association constant, C is the concentration of molecule in solution, R_{ct} (C_o) and R_{ct} (C_i) indicate charge

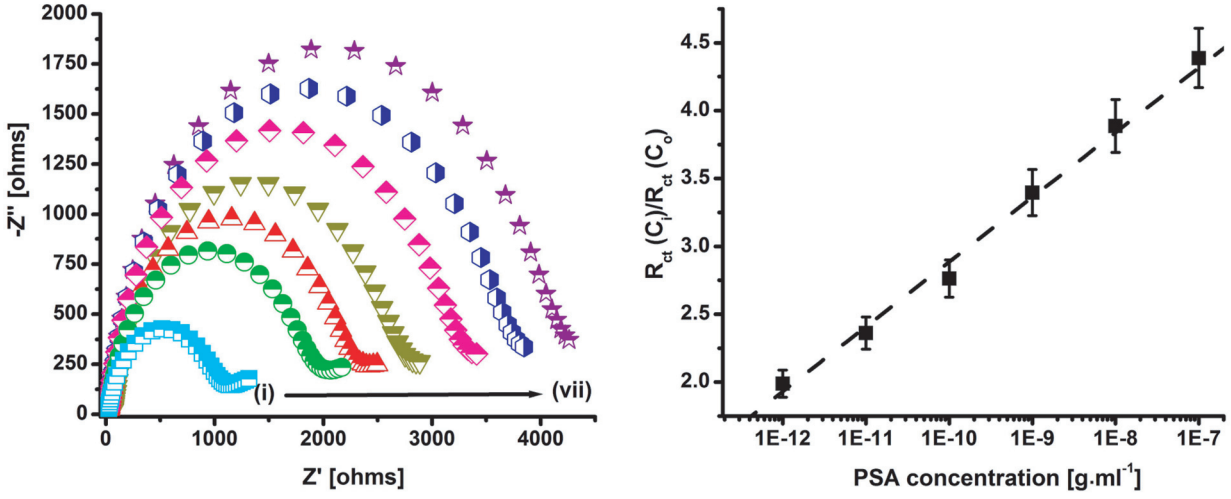

(a) (b)

Figure 5: (a) Nyquist plot of BSA-anti-PSA/Cys/IDE electrode for PSA concentration containing $100\,\text{pg.mL}^{-1}$ of cortisol antibody (i) buffer, (ii) $1\,\text{pg.mL}^{-1}$, (iii) $10\,\text{pg.mL}^{-1}$, (iv) $100\,\text{pg.mL}^{-1}$ (v) $1\,\text{ng.mL}^{-1}$, (vi) $10\,\text{ng.mL}^{-1}$ and (vii) $100\,\text{ng.mL}^{-1}$ and (b) normalized data curve for data obtained from R_{ct} data for different PSA concentration.

transfer resistance of binding sites, without PSA and with desired concentration of PSA, respectively.

Data for R_{ct} was collected from Figure 3, and using (1), the curve was plotted between ΔR_{ct} (C_i)/R_{ct} (C_o) and the concentration of PSA (data not shown). It was found that ΔR_{ct} (C_i)/R_{ct} (C_o) varies linearly with concentration and follows (ΔR_{ct} (C_i)/R_{ct} (C_o)) $= 6.258 + 0.451\ C_{PSA}$, with correlation coefficient of 0.997, and the standard deviation of 0.793. K_a was estimated from the slope of regression equation and found to be $0.451\,\text{mL.g}^{-1}$.

3.3 Specificity studies

The presence of other analytes and proteins in the real sample is a major cause of false results due to nonspecific binding, and thus it needs to be checked. IDE-based BSA-anti-PSA/Cys/IDE electrodes were investigated for their specificity in the detection of PSA. For specificity estimation, EIS measurements were carried out for different concentrations of PSA in PBS containing $100\,\text{pg.mL}^{-1}$ of protein (anti-cortisol) (Figure 5(a)). Figure 5(b) shows the linear variation for normalized R_{ct} values, R_{ct} (C_i)/R_{ct} (C_o), with PSA concentration. Variation can be characterized using R_{ct} (C_i)/R_{ct} (C_o) $= 7.652 + 0.447\ C_{PSA}$, with a correlation coefficient of 0.996 and a sensitivity of $0.447\,\text{mL.g}^{-1}$. The change in sensitivity is attributed to the presence of another protein resulting in some nonspecific binding on surface with PSA. The variation in R_{ct} (C_i)/R_{ct} (C_o) value for different PSA concentrations in the presence of protein was found to be less than 7% for any given PSA concentration. BSA-anti-PSA/Cys/IDE electrodes were also tested for BSA and anti-cortisol in the absence of PSA. The results suggested the selectivity of BSA-anti-PSA/Cys/IDE electrodes with maximum variation of $< 7\%$.

Table 1 shows the comparison of our electrode with other approaches used for PSA estimation. Commercially available ELISA-based test reliably detects PSA in the range of 0.05–$0.005\,\text{ng.mL}^{-1}$ range, however, from Table 1, it is clear that our system is simpler, better and can detect PSA in a wide range with detection limit of $1\,\text{pg.mL}^{-1}$. Such electrochemical measurement design is simple and can be used as point-of-care device.

4 Conclusions

Cysteamine SAM modified IDEs can be used to fabricate an ultrasensitive impedimetric PSA biosensor. Covalently immobilized monoclonal PSA antibody based, BSA-anti-PSA/Cys/IDE electrode exhibited a linear behavior in the concentration range of $1\,\text{pg.mL}^{-1}$–$100\,\text{ng.mL}^{-1}$, with a linear regression coefficient of 0.997 and sensitivity of $0.444\,\text{mL.g}^{-1}$. The association constant for PSA-anti-PSA interaction on electrode was found to be $0.451\,\text{mL.g}^{-1}$. For future work, attempts will be made to improve the specificity of the sensor and to validate the electrode for real samples. The simplicity of design and use of two-electrode-based sensitive detection will be useful for the transformation of PSA detection from lab to point-of-care device.

Acknowledgments This work was partially supported through NSF Award 0700659, Nanoengineered, Manufacturable, Ion-Implantation Seeded Silica Nanowires for Sensitive BioScreening, UF-Moffitt Pilot Award Prostate Cancer Biomarker Study in African American Men, BiTT Award, and an Automated Cell Health Monitoring System (CHMS) Based on Electrical Impedance.

Matrix	Sensing molecule	Transducer	Secondary label	Detector molecule	Incubation time	Linear range	Detection limit	Reference
MUA-APBA conjugate	Anti-PSA-HRP	Amperometric	—	H_2O_2+ thionine	30 min	2–15 and 15–120 $ng.mL^{-1}$	$1.1\,ng.mL^{-1}$	[21]
PANI-poly(1,2-diaminobenzene)	Anti-PSA	EIS	—	—	—	1–100 $pg.mL^{-1}$	$1\,pg.mL^{-1}$	[6]
AuNP	Anti-PSA	LSV	Anti-PSA-biotin and streptavidin-AP	3-IP + $AgNO_3$	200 min	1–10 $ng.mL^{-1}$	$1\,ng.mL^{-1}$	[9]
Cysteamine SAM	Anti-PSA	LSV	SiNP-anti-PSA-AP	AA-P + $AgNO_3$	155 min	1–35 $ng.mL^{-1}$	$0.76\,ng.mL^{-1}$	[26]
PAMAM dendrimer-APEBA SAM	Anti-PSA	CV	Anti-PSA-biotin and avidin-AP	NP	270 min	1–10 $ng.mL^{-1}$	$1\,ng.mL^{-1}$	[24]
Microwell plate	Anti-PSA	Chemilumin escence	Anti-PSA-liposomes encapsulation HPR	Luminol + H_2O_2	120 min	$0.74\,pg.mL^{-1}$– $0.74\,\mu gL^{-1}$	$0.7\,pg.mL^{-1}$	[39]
MWCNT	Anti-PSA	Amperometric	Anti-PSA-HRP	H_2O_2 + 4-TBC	30 min	0–60 μgL^{-1}	$0.08\,\mu gL^{-1}$	[25]
16-MHA, 11-MUOH mixed SAM	cAbPSA-N7	SPR	Anti-PSA-biotin and streptavidin-AuNP		Flow-through	1–100 $ng.mL^{-1}$	$1\,ng.mL^{-1}$	[13]
Cysteamine SAM	Anti-PSA	EIS	—	—	30 min	$1\,pg.mL^{-1}$– $100\,ng.mL^{-1}$	$1\,pg.mL^{-1}$	Present work

16-MHA: 16-mercapto-1-hexadecanoic acid; 11-MUOH: 11-mercapto-1-undecanol; SAM: self-assembled monolayer; SPR: surface plasmon resonance; AuNP: gold nanoparticle; MWCNT: multi-walled carbon nanotube; GCE: glassy carbon electrode; HRP: horseradish peroxidase; H_2O_2: hydrogen peroxide; 4-TBC: 4-*tert*-butylcatechol; MUA: 11-mercaptoundecanoic acid; APBA: 3-aminophenylboronic acid; CV: cyclic voltammetry; PANI: polyaniline; LSV: linear sweep voltammetry; AP: alkaline phosphatase; 3-IP: 3-indoxyl phosphate disodium salt; $AgNO_3$: silver nitrate; AA-P: ascorbic acid 2-phosphate; APEBA: 4-(2-(4-(acetylthio)phenyl)ethynyl)benzoic acid; PAMAM: poly(amidoamine); NP: naphthalene phosphate; SiNP: silica nanoparticle.

Table 1: Comparison of the BSA-anti-PSA/Cys/IDE electrode with the electrodes reported in literature for the PSA estimation.

References

[1] S. K. Arya, G. Chornokur, M. Venugopal, and S. Bhansali, *Antibody functionalized interdigitated μ-electrode (idμe) based impedimetric cortisol biosensor*, Analyst, 135 (2010), 1941–1946.

[2] S. K. Arya, G. Chornokur, M. Venugopal, and S. Bhansali, *Dithiobis(succinimidyl propionate) modified gold microarray electrode based electrochemical immunosensor for ultrasensitive detection of cortisol*, Biosens Bioelectron, 25 (2010), 2296–2301.

[3] S. K. Arya, A. K. Prusty, S. P. Singh, P. R. Solanki, M. K. Pandey, M. Datta, et al., *Cholesterol biosensor based on N-(2-aminoethyl)-3-aminopropyl-trimethoxysilane self-assembled monolayer*, Anal Biochem, 363 (2007), 210–218.

[4] S. K. Arya, S. P. Singh, and B. D. Malhotra, *Electrochemical techniques in biosensors*, in Handbook of Biosensors and Biochips, R. S. Marks, C. R. Lowe, D. C. Cullen, H. H. Weetall, and I. Karube, eds., Wiley-Interscience, New Jersey, 2008, 341–378.

[5] A. J. Bard, M. Stratmann, and P. R. Unwin, *Instrumentation and Electroanalytical Chemistry*, Wiley-VCH, New Jersey, 2003.

[6] A. C. Barton, F. Davis, and S. P. Higson, *Labeless immunosensor assay for prostate specific antigen with picogram per milliliter limits of detection based upon an ac impedance protocol*, Anal Chem, 80 (2008), 6198–6205.

[7] H. Chen, J.-H. Jiang, Y. Huang, T. Deng, J.-S. Li, G.-L. Shen, et al., *An electrochemical impedance immunosensor with signal amplification based on Au-colloid labeled antibody complex*, Sens Actuators B, 117 (2006), 211–218.

[8] J. S. Daniels and N. Pourmand, *Label-free impedance biosensors: opportunities and challenges*, Electroanalysis, 19 (2007), 1239–1247.

[9] V. Escamilla-Gomez, D. Hernandez-Santos, M. B. Gonzalez-Garcia, J. M. Pingarron-Carrazon, and A. Costa-Garcia, *Simultaneous detection of free and total prostate specific antigen on a screen-printed electrochemical dual sensor*, Biosens Bioelectron, 24 (2009), 2678–2683.

[10] C. Fernandez-Sanchez, A. M. Gallardo-Soto, K. Rawson, O. Nilsson, and C. J. McNeil, *Quantitative impedimetric immunosensor for free and total prostate specific antigen based on a lateral flow assay format*, Electrochem Comm, 6 (2004), 138–143.

[11] C. Fernandez-Sanchez, C. J. McNeil, K. Rawson, and O. Nilsson, *Disposable noncompetitive immunosensor for free and total prostate-specific antigen based on capacitance measurement*, Anal Chem, 76 (2004), 5649–5656.

[12] D. A. Healy, C. J. Hayes, P. Leonard, L. McKenna, and R. O'Kennedy, *Biosensor developments: application to prostate-specific antigen detection*, Trends Biotechnol, 25 (2007), 125–131.

[13] L. Huang, G. Reekmans, D. Saerens, J. M. Friedt, F. Frederix, L. Francis, et al., *Prostate-specific antigen immunosensing based on mixed self-assembled monolayers, camel antibodies and colloidal gold enhanced sandwich assays*, Biosens Bioelectron, 21 (2005), 483–490.

[14] K. S. Hwang, J. H. Lee, J. Park, D. S. Yoon, J. H. Park, and T. S. Kim, *In-situ quantitative analysis of a prostate-specific antigen (PSA) using a nanomechanical PZT cantilever*, Lab Chip, 4 (2004), 547–552.

[15] A. Jemal, R. Siegel, E. Ward, T. Murray, J. Xu, C. Smigal, et al., *Cancer statistics, 2006*, CA Cancer J Clin, 56 (2006), 106–130.

[16] E. Katz and I. Willner, *Probing biomolecular interactions at conductive and semiconductive surfaces by impedance spectroscopy: Routes to impedimetric immunosensors, dna-sensors, and enzyme biosensors*, Electroanalysis, 15 (2003), 913–947.

[17] J. H. Lee, K. S. Hwang, J. Park, K. H. Yoon, D. S. Yoon, and T. S. Kim, *Immunoassay of prostate-specific antigen (PSA) using resonant frequency shift of piezoelectric nanomechanical microcantilever*, Biosens Bioelectron, 20 (2005), 2157–2162.

[18] X. Li, L. Shen, D. Zhang, H. Qi, Q. Gao, F. Ma, et al., *Electrochemical impedance spectroscopy for study of aptamer-thrombin interfacial interactions*, Biosens Bioelectron, 23 (2008), 1624–1630.

[19] Y. Y. Lin, J. Wang, G. Liu, H. Wu, C. M. Wai, and Y. Lin, *A nanoparticle label/immunochromatographic electrochemical biosensor for rapid and sensitive detection of prostate-specific antigen*, Biosens Bioelectron, 23 (2008), 1659–1665.

[20] D. Liu, R. K. Perdue, L. Sun, and R. M. Crooks, *Immobilization of DNA onto poly(dimethylsiloxane) surfaces and application to a microelectrochemical enzyme-amplified DNA hybridization assay*, Langmuir, 20 (2004), 5905–5910.

[21] S. Liu, X. Zhang, Y. Wu, Y. Tu, and L. He, *Prostate-specific antigen detection by using a reusable amperometric immunosensor based on reversible binding and leasing of HRP-anti-PSA from phenylboronic acid modified electrode*, Clin Chim Acta, 395 (2008), 51–56.

[22] J. R. Macdonald and W. B. Johnson, *Fundamentals of impedance spectroscopy*, in Impedance Spectroscopy: Theory, Experiment, and Applications, E. Barsoukov and J. R. Macdonald, eds., John Wiley & Sons, New Jersey, 2nd ed., 2005, 1–8.

[23] K. Maruyama, H. Ohkawa, S. Ogawa, A. Ueda, O. Niwa, and K. Suzuki, *Fabrication and characterization of a nanometer-sized optical fiber electrode based on selective chemical etching for scanning electrochemical/optical microscopy*, Anal Chem, 78 (2006), 1904–1912.

[24] M. O. Namgung, S. K. Jung, C. M. Chung, and S. Y. Oh, *Electrochemical immunosensor for prostate-specific antigen using self-assembled oligophenylethynylenethiol monolayer containing dendrimer*, Ultramicroscopy, 109 (2009), 907–910.

[25] N. V. Panini, G. A. Messina, E. Salinas, H. Fernandez, and J. Raba, *Integrated microfluidic systems with an immunosensor modified with carbon nanotubes for detection of prostate specific antigen (PSA) in human serum samples*, Biosens Bioelectron, 23 (2008), 1145–1151.

[26] B. Qu, X. Chu, G. Shen, and R. Yu, *A novel electrochemical immunosensor based on colabeled silica nanoparticles for determination of total prostate specific antigen in human serum*, Talanta, 76 (2008), 785–790.

[27] J. Ramon-Azcon, E. Valera, A. Rodriguez, A. Barranco, B. Alfaro, F. Sanchez-Baeza, et al., *An impedimetric immunosensor based on interdigitated microelectrodes (idμe) for the determination of atrazine residues in food samples*, Biosens Bioelectron, 23 (2008), 1367–1373.

[28] A. Rodriguez, E. Valera, J. R. Azcon, F. J. Sanchez, M. P. Marco, and L. M. Castaner, *Single frequency impedimetric immunosensor for atrazine detection*, Sens Actuators B, 129 (2008), 921–928.

[29] P. Sarkar, P. S. Pal, D. Ghosh, S. J. Setford, and I. E. Tothill, *Amperometric biosensors for detection of the prostate cancer marker (PSA)*, Int J Pharma, 238 (2002), 1–9.

[30] S. A. Soper, K. Brown, A. Ellington, B. Frazier, G. Garcia-Manero, V. Gau, et al., *Point-of-care biosensor systems for cancer diagnostics/prognostics*, Biosens Bioelectron, 21 (2006), 1932–1942.

[31] R. Stevenson, A. Ingram, H. Leung, D. C. McMillan, and D. Graham, *Quantitative SERRS immunoassay for the detection of human PSA*, Analyst, 134 (2009), 842–844.

[32] L. C. Su, R. C. Chen, Y. C. Li, Y. F. Chang, Y. J. Lee, C. C. Lee, et al., *Detection of prostate-specific antigen with a paired surface plasma wave biosensor*, Anal Chem, 82 (2010), 3714–3718.

[33] I. Szymanska, H. Radecka, J. Radecki, and R. Kaliszan, *Electrochemical impedance spectroscopy for study of amyloid β-peptide interactions with (−) nicotine ditartrate and (−) cotinine*, Biosens Bioelectron, 22 (2007), 1955–1960.

[34] E. Valera, J. R. Azcon, A. Rodriguez, L. M. Castaner, F. J. Sanchez, and M. P. Marco, *Impedimetric immunosensor for atrazine detection using interdigitated μ-electrodes (IDμE's)*, Sens Actuators B, 125 (2007), 526–537.

[35] M. Varshney and Y. Li, *Interdigitated array microelectrodes based impedance biosensors for detection of bacterial cells*, Biosens Bioelectron, 24 (2009), 2951–2960.

[36] J. Wang, *Electrochemical biosensors: Towards point-of-care cancer diagnostics*, Biosens Bioelectron, 21 (2006), 1887–1892.

[37] R. Wang, Y. Wang, K. Lassiter, Y. Li, B. Hargis, S. Tung, et al., *Interdigitated array microelectrode based impedance immunosensor for detection of avian influenza virus H5N1*, Talanta, 79 (2009), 159–164.

[38] Y. Wang, A. Brunsen, U. Jonas, J. Dostalek, and W. Knoll, *Prostate specific antigen biosensor based on long range surface plasmon-enhanced fluorescence spectroscopy and dextran hydrogel binding matrix*, Anal Chem, 81 (2009), 9625–9632.

[39] Y. Zheng, H. Chen, X. P. Liu, J. H. Jiang, Y. Luo, G. L. Shen, et al., *An ultrasensitive chemiluminescence immunosensor for PSA based on the enzyme encapsulated liposome*, Talanta, 77 (2008), 809–814.